

Eva Corey ORCID iD: 0000-0002-9244-3807

John Isaacs ORCID iD: 0000-0002-3854-4658

Gail Risbridger ORCID iD: 0000-0003-3089-4028

Establishing a cryopreservation protocol for patient-derived xenografts of prostate cancer

Laura H. Porter^{1*}, Mitchell G. Lawrence^{1,2*}, Hong Wang¹, Ashlee K Clark¹, Andrew Bakshi^{1,2,3}, Daisuke Obinata¹, David Goode^{2,3,4}, Melissa Papargiris^{1,5}, MURAL¹, David Clouston⁶, Andrew Ryan⁶, Sam Norden⁶, Eva Corey⁷, Peter S. Nelson^{7,8,9}, John T. Isaacs¹⁰, Jeremy Grummet^{11,12}, John Kourambas¹³, Shahneen Sandhu^{4,14,15}, Declan G. Murphy^{4,12,16}, David Pook^{1,17}, Mark Frydenberg^{1,11,12,18}, Renea A. Taylor^{1,19*}, Gail P. Risbridger^{1,2*}

¹Monash Partners Comprehensive Cancer Consortium, Monash Biomedicine Discovery Institute, Prostate Cancer Research Group, Department of Anatomy and Developmental Biology, Monash University, Clayton, Victoria, Australia, 3800.

²Cancer Research Program, Cancer Research Division, Peter MacCallum Cancer Centre, University of Melbourne, Melbourne, Victoria, Australia, 3000.

³Computational Cancer Biology Program, Peter MacCallum Cancer Centre, Melbourne, Victoria, Australia, 3000.

⁴Sir Peter MacCallum Department of Oncology, University of Melbourne, Victoria, Australia, 3000.

This is the author manuscript accepted for publication and undergone full peer review but has not been through the copyediting, typesetting, pagination and proofreading process, which may lead to differences between this version and the [Version of Record](#). Please cite this article as [doi: 10.1002/pros.23839](https://doi.org/10.1002/pros.23839).

⁵Australian Prostate Cancer Bioresource, Victoria Node, Monash University, Clayton, Victoria, Australia, 3800.

⁶TissuPath, Mount Waverley, Victoria, Australia, 3149.

⁷Department of Urology, University of Washington, Seattle, Washington, USA, 98195.

⁸Division of Human Biology, Fred Hutchinson Cancer Research Center, Seattle, Washington, USA, 98109

⁹Department of Pathology, University of Washington, Seattle, Washington, USA, 98195.

¹⁰Department of Oncology, Prostate Cancer Program, The Sidney Kimmel Comprehensive Cancer Center at Johns Hopkins, The Johns Hopkins University School of Medicine, Baltimore, Maryland, USA, 21287.

¹¹Department of Surgery, Central Clinical School, Monash University, Clayton, Victoria, Australia, 3800

¹²Epworth Healthcare, Richmond, Victoria, Australia, 3121

¹³Department of Medicine, Monash Health, Casey Hospital, Berwick, Victoria, Australia, 3806.

¹⁴Division of Cancer Medicine, Peter MacCallum Cancer Centre, University of Melbourne, Victoria, Australia, 3000.

¹⁵Cancer Tissue Collection After Death (CASCADE) Program, Peter MacCallum Cancer Centre, University of Melbourne, Victoria, Australia, 3000.

¹⁶Division of Cancer Surgery, Peter MacCallum Cancer Centre, University of Melbourne, Victoria, Australia, 3000

¹⁷Medical Oncology, Monash Health, Clayton, Victoria, Australia, 3800.

¹⁸Australian Urology Associates, Melbourne, Victoria, Australia, 3000.

¹⁹Monash Partners Comprehensive Cancer Consortium, Monash Biomedicine Discovery Institute, Prostate Cancer Research Group, Department of Physiology, Monash University, Clayton, Victoria, Australia, 3800.

**Authors contributed equally to this work*

Address for correspondence:

Professor Gail Risbridger, PhD

Monash Biomedicine Discovery Institute, Department of Anatomy and Developmental Biology

19 Innovation Walk, Clayton VIC Australia 3800

Phone: (03) 9902 9558

Email: gail.risbridger@monash.edu

Running Title: Cryopreserving prostate cancer PDXs

Disclosure Statement: The authors do not have conflicts of interest to declare

Abstract

Background: Serially-transplantable patient-derived xenografts (PDXs) are invaluable preclinical models for studying tumor biology and evaluating therapeutic agents. As these models are challenging to establish from prostate cancer specimens, the ability to preserve them through cryopreservation has several advantages for ongoing research. Despite this, there is still uncertainty about the ability to cryopreserve PDXs of prostate cancer. This study compared three different cryopreservation protocols to identify a method that can be used to reproducibly cryopreserve a diverse cohort of prostate cancer PDX models.

Methods: One serially-transplantable prostate cancer PDX from the Melbourne Urological Research Alliance (MURAL) cohort was used to compare three cryopreservation protocols: slow freezing in fetal calf serum with 10% DMSO, fetal calf serum with 10% DMSO supplemented with the ROCK inhibitor Y-27632 and vitrification. The efficiency of the slow freezing protocols were then assessed in 17 additional prostate cancer PDXs. Following cryopreservation, PDXs were re-established in host mice that were either intact and supplemented with testosterone or castrated. Graft take rate, tumor growth, histological features and transcriptome profiles before and after cryopreservation were compared.

Results: Slow freezing maintained the viability and histological features of prostate cancer PDXs, and the addition of a ROCK inhibitor increased their growth following cryopreservation. Using the slow freezing method, we re-established 100% of PDXs grown in either testosterone-supplemented or castrated host mice. Importantly, the long-term tumor growth rate and transcriptome profile were maintained following cryopreservation.

Conclusion: This study has identified a protocol to reliably cryopreserve and re-establish a diverse cohort of serially-transplantable PDXs of prostate cancer. This work has the potential to significantly improve the practicality of maintaining PDX models. Cryopreservation may also increase the accessibility of these important resources and provide new opportunities for preclinical studies on a broader spectrum of prostate tumors.

Key words

Patient-derived xenografts, freezing, castration-resistant prostate cancer, localized prostate cancer

Introduction

Patient-derived xenografts (PDXs) are crucial preclinical models for studying tumor biology and testing new therapies. PDXs retain the features of the original tumor, represent diverse tumors from different stages of disease progression and reflect the heterogeneity of tumors seen in the clinic. Although serially transplantable PDXs are available for many tumor types [1], they are challenging for prostate cancer. This is evident by the low numbers of prostate cancer PDXs in international consortia, including the EurOPDX Consortium, JAX Laboratories and BioMedical Research PDX encyclopedia, where prostate cancer PDXs constitute only 1% of the collection in some cases [1-3]. To address this problem, academic groups developed a repertoire of serially-transplantable PDX of prostate cancer [4], resulting in over 100 authenticated PDXs, including those from the Living Tumor Laboratory, the LuCaP series, the MDA PCa series, the Johns Hopkins University cohort, our recently published collection from the Melbourne Urological Research Alliance (MURAL), and others [4-7]. The take rates for establishing these serially-transplantable PDX

were 10-40% and they often had long latency times of up to 12 months after initial grafting [4]. Therefore, given the difficulty in establishing serially transplantable PDXs, it is important to maximize their preservation and maintain them for ongoing prostate cancer research.

As the number of prostate cancer PDXs increases, the process of maintaining them becomes more laborious and time-consuming. PDXs are often maintained by continually re-passaging them into new host mice, which can be as often as every few weeks for fast growing tumors [5-7]. Therefore, the ability to store PDXs through cryopreservation would decrease the workload of maintaining them. It could also provide backup stocks of low-passage PDXs in case tumor features begin to diverge over time or grafts become contaminated. Cryopreserved PDXs may also be faster and easier to transport than host mice, increasing the opportunities for collaborative research and expanding the diversity of tumors available for preclinical testing. Despite these potential benefits, there is still uncertainty about the ability to re-establish prostate cancer PDXs after cryopreservation. There has been some reports of successfully cryopreserving prostate cancer PDXs [7,8]; however, no formal comparison of different cryopreservation protocols and their success rates has been published.

Various protocols are used to cryopreserve human cells and tissues. The most common method of cryopreservation, including for cultured prostate cancer cells [9], is slow freezing using the traditional cryoprotectant dimethyl sulfoxide (DMSO). This method may be improved by the addition of the Rho-associated kinase (ROCK) inhibitor Y-27632, as adding it to cryopreservation media during or after cryopreservation improves the recovery of embryonic stem cells, breast cancer cells

and intestinal organoids, likely by preventing anoikis [10-15]. Another method of cryopreservation is vitrification, where tissues are briefly immersed in high concentrations of cryoprotectants before being rapidly frozen in liquid nitrogen. Vitrification maintains the viability and proliferative capacity of ovarian and testicular tissue [16-18], so may be another approach for cryopreserving prostate cancer PDXs. In this study, we compared slow freezing and vitrification to establish a protocol for reproducibly cryopreserving and regenerating established PDXs. We found that slow freezing maintains the viability of prostate cancer PDXs, and the addition of the ROCK inhibitor increases their growth following cryopreservation. Using these protocols, we could re-establish 100% of the diverse PDXs that were cryopreserved. Therefore, these methods have the potential to significantly improve the practicality of maintaining and disseminating prostate cancer PDXs.

Materials and Methods

Patient specimens

Prostate cancer tissue was collected from four sources: 1) localized prostate cancer specimens from patients undergoing radical prostatectomy; 2) surgical specimens of symptomatic metastases from patients with castrate-resistant prostate cancer (CRPC), 3) biopsies of metastases from patients with CRPC and; 4) rapid autopsy samples from patients with CRPC through the CASCADE program [19]. Informed, written consent was obtained from participants prior to tissue collection according to human ethics approval from the Cabrini Institute (03-14-04-08), Monash University (1636), Peter MacCallum Cancer Centre (15/98, 97_27) and the Johns Hopkins University School of Medicine IRB.

Patient-derived xenografts

In conducting research using animals, the investigators adhered to the laws of the United States and regulations of the Department of Agriculture. Experiments with the MURAL cohort of PDXs were conducted according to animal ethics approval from Monash University (MARF/2014/085 and MARF/2018/087). Serially-transplantable PDXs of localized and metastatic prostate cancer were established and characterized by MURAL, as previously reported [5,20]. In brief, tumor tissue was implanted under the renal capsule of 6-8 week old male non-obese diabetic severe-combined immune-deficient gamma (NSG) mice. At the time of grafting, a 5 mm testosterone pellet was implanted subcutaneously to supplement host testosterone levels. The abdomens of the mice were palpated weekly to monitor tumor growth. Grafts were transplanted into new host mice if they reached approximately 1 cm³ or due to animal ethics welfare considerations. PDXs were defined as serially transplantable if they could be grown for at least three generations with at least a 10-fold increase in graft volume each generation. Once serially transplantable lines were established, they were maintained subcutaneously or under the renal capsule. Whilst all PDX lines were initially established in host mice supplemented with testosterone, four sublines have been established by serially-passaging the tumors in castrated host mice. The identity of PDXs was periodically authenticated by profiling short tandem repeats with the GenePrint 10 System (Promega) using germline DNA or early generation PDXs as controls. Immunohistochemistry was also performed using the human-specific antibody for the luminal cell marker cytokeratin 8/18 to confirm tumor was of human origin.

The PDXs of Supplemental Table 1 were established at Johns Hopkins School of Medicine, Baltimore MD, except CWR22 and its androgen independent CWR22-CR

variant. The original androgen-responsive CWR22 tumor was established at Case Western Reserve and its androgen independent CRR22-CR variant was established at Hopkins by serial passage in castrated male nude mice, as previously described [21,22]. The other PDXs were established from tumor specimens from metastatic CRPC patients with signed, informed consent. Specimens were obtained from either resection of distant metastases at rapid autopsy to limit warm ischemic time as much as possible (aiming for 4-8 h after death) or from biopsy of a metastasis before death. Harvested tumor tissues were evaluated by pathologists and tumor pieces were then prepared for implantation. All animal procedures were approved by the Johns Hopkins University School of Medicine Institutional Animal Care and Use Committee. NOD-SCID, triple immune-deficient NOG or NSG adult male mice, obtained from the Sidney Kimmel Comprehensive Cancer Center (SKCCC) Animal Core Facility, were used for tissue implantation. Grafts were implanted at subcutaneous sites as indicated in Supplemental Table 1.

Cryopreservation of patient-derived xenograft lines

To compare cryopreservation methods, PDX 27.1 was cryopreserved using three different cryopreservation protocols. PDX tissue was harvested at the end of generation one and dissected into 4 mm³ pieces. As freshly grafted controls, three pieces were immediately re-grafted under the renal capsule of host mice with testosterone implants. The remaining tissue pieces were cryopreserved using three cryopreservation protocols. For two protocols, up to six pieces of tumor were placed in 1 ml of cryopreservation media and frozen at a rate of 1°C/minute in a NalgeneTM Mr Frosty Cryo 1°C Freezing container (Thermo Scientific) at -80°C. Cryopreservation media was supplemented with either fetal calf serum (FCS) and 10% DMSO, designated FCS or with FCS, 10% DMSO and 5 µM of the ROCK

inhibitor Y-27632 (Sigma Aldrich), designated FCS-R, as previously described [11]. The FCS protocol was used for all PDXs in Supplemental Table 1 from Johns Hopkins University. The third protocol, vitrification, was previously described [18]. In brief, tissue was pre-treated with an equilibrium solution of RPMI 1640 containing 10% FCS, 7.5% DMSO, 7.5% ethylene glycol (Sigma Aldrich) and 0.25 M sucrose (Sigma Aldrich). Each 4 mm³ tissue piece was placed in a 1.5 ml cryovial containing 1 ml of equilibrium solution for 10 minutes at room temperature. The equilibrium solution was aspirated and replaced with 1 ml of a vitrification solution of RPMI 1640 containing 20% FCS, 15% DMSO, 15% ethylene glycol and 0.5 M sucrose. Following incubation for 5 minutes at room temperature, the vitrification solution was aspirated, and the tumors were snap frozen in liquid nitrogen. Once frozen, all cryopreserved tissue was stored in liquid nitrogen for three weeks before being rapidly thawed at 41°C. Cryopreservation media was slowly diluted with RPMI 1640 supplemented with 10% FCS, 1% penicillin-streptomycin, 25 mM HEPES sodium salt and 10 nM testosterone (Sigma Aldrich) and tissue pieces were grafted into host mice.

To compare the growth of PDX lines after cryopreservation, 9 PDX lines were cryopreserved at generation 1 to 16 before being re-grafted into host mice either subcutaneously or under the renal capsule. Tissue was cryopreserved in FCS-R frozen at a rate of 1°C/minute in a NalgeneTM Mr Frosty Cryo 1°C Freezing. Tissue was stored in liquid nitrogen for between 48-940 days before being rapidly thawed at 41°C and re-grafted into host mice.

Graft analysis

At collection, grafts were fixed in 10% formalin and embedded in paraffin. Tumor pathology was determined by hematoxylin and eosin staining. Staining was also performed for androgen receptor (A9853, Sigma Aldrich, Rabbit IgG, 2.0 µg/ml), cytokeratin 8/18 (NCL-L-5D3, Novocastra, Mouse IgG1, 0.26 µg/ml), cleaved caspase 3 (9661, Cell Signalling, Rabbit IgG, 0.16 µg/ml), Ki67 (MM1, Novocastra, Mouse IgG1, 0.2 µg/ml) and prostate specific antigen (A0562, DAKO, Rabbit IgG, 1 µg/ml). All immunohistochemistry was performed by the Leica BOND-MAX-TM automated system (Leica Microsystems). The BOND Refine Red Detection Kit (Leica Microsystems) was used for cytokeratin 8/18, whilst the BOND Refine Detection Kit (Leica Microsystems) was used for all other antibodies. Antigen retrieval was performed using BOND TM epitope retrieval 1 for androgen receptor and BOND TM epitope retrieval 2 for all other antibodies, with the exception of prostate specific antigen which had no epitope retrieval.

To determine the number of proliferative and apoptotic cells, immunohistochemistry was conducted for Ki67 and cleaved caspase 3 respectively on three sections per graft. Slides were imaged using ScanScope AT Turbo Slide Scanner (Aperio). The number of Ki67-positive and cleaved caspase 3-positive cells was determined using ImageScope analysis software (Aperio) and expressed as a percentage of the total number of cells counted.

RNA analysis

RNA was isolated using the miRNeasy Mini Kit (Qiagen). RNA quality was assessed using the RNA 6000 Nano Kit on the BioAnalyser (Agilent) and the Nanodrop was used to determine RNA quality and quantity. RNA sequencing libraries were prepared

using NEBNext Ultra II Directional RNA library preparation kit and paired end 75 bp RNA sequencing reads were generated using Illumina NexSeq. 500. Raw sequencing reads were processed using ‘Seqliner’ (<http://www.seqliner.org>). In brief, CASAVA 1.8.2 (Illumina) was used for base calling. Reads were quality checked by FastQC. Reads were aligned to both the human (GRCh37) and mouse (mm10) references genomes using HISAT2 (version 2.0.4)[23]. Aligned human and mouse reads were separated using Xenomapper (version 1.0.1)[24]. The primary human specific bam files from Xenomapper were kept. Expression counts for each gene were determined using featureCounts from Rsubread package (version 1.30.9)[25]. Genes that did not have greater than 1 CPM reads across at least two samples were filtered out. Data was normalized using edgeR (3.22.5)[26]. We calculated the Pearson correlation between the log2 counts per million for all genes after filtering.

Statistical analysis

All data were expressed as mean \pm standard error of the mean. Statistical significance was determined using one-way analysis of variance with post hoc Dunnett’s test. Statistical significance was set at $p < 0.05$. Statistical analysis was conducted using GraphPad Prism 6 software (GraphPad Software Inc).

Results

We have previously established serially-transplantable PDXs of prostate cancer through the MURAL platform [5]. To determine whether these PDXs could be cryopreserved and then re-established from thawed tissue, we compared the effectiveness of different cryopreservation techniques. For these experiments, we selected PDX 27.1, a tumor with moderate growth rate established from the dural metastasis of a patient with CRPC. PDX tissue at generation one was cryopreserved

using three protocols: slow freezing in fetal calf serum with 10% DMSO (FCS), fetal calf serum with 10% DMSO supplemented with a ROCK inhibitor (FCS-R) and vitrification (**Fig. 1A**). All cryopreserved tissues were thawed using a rapid-thaw protocol before being re-grafted into host mice. The take rate and graft volume of cryopreserved tissues were compared to fresh tissue controls, which were directly re-grafted and grown in host mice for six weeks (**Fig. 1A**). Both slow freezing protocols maintained the viability of prostate cancer cells, with 100% take rate of grafts after cryopreservation in FCS or FCS-R (**Table 1**). Notably, the average graft volume was not significantly different following slow freezing in FCS ($16.3 \pm 2.9 \text{ mm}^3$; $P = 0.09$) nor FCS-R ($25.1 \pm 5.1 \text{ mm}^3$; $P = 0.8$) compared to freshly grafted controls ($29.4 \pm 3.0 \text{ mm}^3$) after six weeks in host mice (**Fig. 1B**). However, among these cryopreservation protocols, average graft volume was highest following cryopreservation in FCS-R (**Fig. 1B**), suggesting that the addition of the ROCK inhibitor to the cryopreservation media improved PDX growth. Vitrification was less successful than slow freezing, with only 50% take rate (**Table 1**) and significantly reduced graft volume compared to control ($2.3 \pm 0.9 \text{ mm}^3$ vs $29.4 \pm 3.0 \text{ mm}^3$; $P < 0.001$; **Fig. 1B**). Thus, slow freezing maintains the viability of prostate cancer PDXs, and the addition of the ROCK inhibitor increases their growth following cryopreservation.

Since PDX growth was maintained after slow freezing in FCS and FCS-R, we assessed whether they retained their histopathological features. Hematoxylin and eosin staining showed that grafts cryopreserved in FCS and FCS-R retained the morphology of the original PDX (**Fig. 1C**). The expression of cytokeratin 8/18, androgen receptor and prostate specific antigen were also consistent (**Fig. 1C**). The percentage of proliferating cells, marked by Ki67, was significantly increased in FCS ($69.3 \pm 1.1\%$; $p < 0.05$) and FCS-R ($71.3 \pm 3.4\%$; $p < 0.01$) cryopreserved grafts

compared to freshly grafted controls ($57.7 \pm 2.9\%$; **Fig. 1C,D**), possibly due to the slightly smaller volume of grafts that were re-established after slow freezing (**Fig. 1B**). There was no significant difference in the number of apoptotic cleaved caspase 3-positive cells (**Fig. 1C,E**). Thus, prostate cancer viability and histopathology were maintained in PDXs following slow freezing.

We next examined whether the FCS-R protocol was effective for a diverse range of other prostate cancer PDXs by measuring their take rates after cryopreservation. Nine PDXs from the MURAL collection were cryopreserved, including the PDX used in the previous experiments. The cohort included three PDXs of castrate-sensitive localized prostate cancer and six PDXs of metastatic CRPC growing in intact host mice supplemented with testosterone [5]. Three of the CRPC PDXs were also serially passaged in castrated host mice (**Table 1**). PDX tissues were cryopreserved generations 1-16 and stored in liquid nitrogen for 48-940 days before being rapidly thawed and re-grafted into host mice (**Table 1**). All PDXs were successfully re-established after cryopreservation with an average take rate of 86% (range 13-100%) (**Table 1**). Notably, all PDXs had a 100% take rate except two PDXs of localized prostate cancer, where only 13% (PDX 156) and 17% (PDX 167.1) of grafts re-grew tumor following cryopreservation (**Table 1**). The PDXs of CRPC had the same take rate in testosterone-supplemented and castrated host mice. Collectively, these data show that the FCS-R protocol can be used to re-establish a diverse range of PDXs from localized and metastatic prostate cancer.

Since the traditional FCS protocol was also effective for PDX 27.1, we verified that other PDXs could be re-established after being cryopreserved with this technique. Nine PDXs of localized and metastatic prostate cancer were cryopreserved at Johns

Hopkins University (Supplemental **Table S1**). This cohort included seven PDXs of metastatic CRPC and the classical CWR22 and CWR22-CR PDXs originally established from a primary prostate tumor [4,27]. Every PDX could be re-established under standard grafting conditions in either intact or castrate host mice, with an average take rate of 65% (range 20-100%) versus 95% (range 80-100%) for fresh tissues (**Table S1**). This confirms that slow freezing is a reliable method of cryopreservation for prostate cancer PDXs.

In addition to engraftment take rate, it is important that PDXs maintain the same growth rate across time. To assess long-term growth, PDXs cryopreserved using the FCS-R protocol and grown in testosterone-supplemented conditions were serially-transplanted between host mice (**Fig. 2A-I**). The average time per generation before cryopreservation was compared to the first transition generation following cryopreservation and all subsequent generations after cryopreservation (**Fig. 2A-J**). Out of the nine PDXs, only two PDXs of localised prostate cancer, PDX 156 and PDX 167.1, had a lag in their growth rate after cryopreservation, demonstrated by a longer transition generation (**Fig. 2G,H**). This is consistent with their decreased engraftment rate following cryopreservation (**Table 1**) and suggests that certain PDXs may take longer to re-establish than others. However, this was only transient, and no significant difference was observed in the average time per generation before and after cryopreservation across the nine PDXs (**Fig. 2J**). Thus, the FCS-R cryopreservation protocol maintained the long-term growth rate of PDXs.

We also investigated whether these PDXs maintained the same histopathological and transcriptional profile across time. The histopathological features of the PDXs cryopreserved with FCS-R and grown in host mice supplemented with testosterone

Author Manuscript

were maintained, as determined by hematoxylin and eosin staining (**Fig. 3A**). RNA sequencing was performed on four generations of tissue from PDX 167.2, which is maintained in host mice supplemented in testosterone and was re-established after cryopreservation at generation 12 (**Table 1**). RNA sequencing was performed on samples from before cryopreservation (generations 1, 5 and 8) and two passages after cryopreservation (generation 14). There was a high level of similarity between the transcriptome profile at generation 14 compared to generations 1, 5 and 8, with correlation coefficients of $r=0.91$, $r=0.98$ and $r=0.99$ respectively (**Fig. 3B,C**). This was consistent with variability between the transcription profiles of generations prior to cryopreservation (**Fig. 3C**). Therefore, the FCS-R method of cryopreservation maintains the viability, growth rate, histopathology and transcriptome profile of prostate cancer PDXs.

Discussion

Serially-transplantable PDXs of prostate cancer are technically challenging models that are a valuable resource for pre-clinical testing [4]. The ability to reproducibly cryopreserve and re-establish PDXs would considerably improve their maintenance and distribution within the research community. Therefore, we formally compared three cryopreservation protocols to determine suitable methods for freezing PDXs of prostate cancer. We found that traditional slow freezing with DMSO maintained tissue viability and histopathology and that adding a ROCK inhibitor enhanced the initial re-growth of tumors compared to other cryopreservation methods. These slow freezing protocols were effective for a diverse cohort of PDXs, grown either subcutaneously or under the renal capsule, including those grown in castrated host mice. Importantly, after the cryopreserved PDXs were re-established, their long-term

tumor growth rate was maintained, including PDXs of localized prostate cancer. We have therefore shown that prostate cancer PDXs can be reproducibly re-established after cryopreservation. This provides new opportunities for sharing these precious resources and reducing the time and costs of continuous passaging.

Despite the increasing use of PDXs for preclinical prostate cancer research, there are only a few reports of cryopreserving them. From the Living Tumor Laboratory series of prostate cancer PDXs, Lin et al. (2014) reported a 95% recovery rate for small pieces of xenograft tissue frozen in DMSO and stored in liquid nitrogen [7]. Another study reported that a PDX derived from metastatic CRPC, designated 'C5', can be re-established with a 90% success rate following cryopreservation in CryoSafe Medium [8]. Although these studies did not describe the precise cryopreservation protocols, including the rates of freezing, there are likely to be several methods for successfully cryopreserving PDX tissue. This prompted us to compare different cryopreservation protocols. Using PDX 27.1, established from the dural metastasis of a patient with CRPC, we found that slow freezing was more effective than vitrification.

Furthermore, slow freezing maintained the viability of a wide variety of PDXs across two research institutes. By tracking the growth of PDXs for multiple generations, in several cases for over 500 days, we also confirmed that the long-term tumor growth rate of PDXs is maintained after cryopreservation.

Whilst both FCS and FCS-R slow freezing protocols could be used to successfully re-establish PDXs, adding the ROCK inhibitor increased the initial growth of PDX 27.1 compared to other cryopreservation methods. ROCK inhibitors have been used to improve culturing of numerous cell types, because they promote increased cell survival, proliferation and adhesion, predominantly by altering actin/myosin

Author Manuscript

cytoskeleton activity and the E-cadherin-dependent apoptotic pathway [11,13-15,28]. These effects are reversed following removal of the ROCK inhibitor from the culture medium, allowing for the temporary modulation of cell behaviour [13,29]. Since several studies have shown that ROCK inhibitors do not alter the gene expression, pluripotent phenotype and differentiation potential of human embryonic and induced pluripotent stem cells, and they are routinely used in stem cell cultures [12-14,28]. In our study, the long-term growth rates, histopathology and transcriptomic profile of PDXs were concordant before and after cryopreservation. This suggests that slow freezing with the ROCK inhibitor does not cause long-term changes to the phenotype of prostate cancer PDXs.

A limitation of cryopreservation is the lower re-engraftment rate of some PDXs. For example, among the PDXs cryopreserved with FCS-R, two PDXs of treatment naïve localized prostate cancer had lower take rates than the other tumors and reduced growth rates in the first-generation following cryopreservation. This is consistent with our experience that it is often more difficult to establish and maintain PDXs from treatment naïve primary prostate cancer compared to metastatic specimens [30,31]. It is therefore promising that we could re-establish these localized prostate cancer PDXs following cryopreservation, albeit with a lower re-engraftment rate. Yet, it is possible that some prostate cancer PDXs may be too difficult to cryopreserve. Therefore, for new PDX models it would be prudent to cryopreserve multiple samples and confirm that they can be re-established.

The focus of this study was to cryopreserve established, actively-growing PDXs; however, an alternative approach would be to cryopreserve patient tissue before engraftment at the time of specimen collection. This strategy has only been reported

in a few cases for prostate cancer specimens, with limited success rates. CRPC specimens obtained from autopsy were snap-frozen using liquid nitrogen before xenografting, but the subsequent graft survival rate was only 5% [32]. Another study reported that tumor tissue from one specimen was maintained in xenografts for up to one month following cryopreservation prior to engraftment; however, these grafts were not serially-transplanted [33]. Unfortunately, we have not been able to establish PDXs from cryopreserved fresh specimens (data not shown), although we have only attempted a limited number of samples that were predominantly from low-grade localised prostate cancer. Since a crucial aspect of establishing PDXs of prostate cancer is obtaining viable tumor tissue [6,20,34], our standard protocol is to graft specimens as soon as possible after collection to maximize their success rate. However, once the tissue is actively growing in host mice, we are able to cryopreserve the PDX tumor for long-term storage as early as the first generation.

Conclusion

This study identified a cryopreservation protocol for reproducibly freezing and re-establishing serially-transplantable PDXs of prostate cancer. Slow freezing maintains the viability of a diverse cohort of PDXs grown in different host conditions, while adding a ROCK inhibitor increases the initial growth rate. The ability to cryopreserve PDXs of prostate cancer will improve their maintenance and provide frozen biobanks of these important preclinical models. The ability to reliably cryopreserve PDXs will foster collaborative exchange between researchers, providing new opportunities to use a broader spectrum of prostate tumors in preclinical studies.

Acknowledgements

We thank the patients and families who generously supported this research by consenting to provide tissue. We thank Wallace Crellin for invaluable advice, the Australian Prostate Cancer BioResource for specimen collection, the Melbourne Urological Research Alliance for providing PDXs and the Monash Histology Platform for technical assistance. This work was supported by the U.S. Department of Defense, through the Prostate Cancer Research Program under Award No. W81XWH1810347, W81XWH1810348 and W81XWH1810349. Opinions, interpretations, conclusions and recommendations are those of the authors and are not necessarily endorsed by the Department of Defense. This research was also supported by funding from the National Health and Medical Research Council (Project grants 1059855, 1077799, 1138242, 1140222 and 1156570; Fellowship to GPR 1002648), the Victorian Government through the Victorian Cancer Agency (Fellowships to RAT MCRF15023 and MGL MCRF18017; CAPTIV program), the Endocrine Society of Australia (Research Seed Grant to MGL), Monash University Faculty of Medicine, Nursing and Health Sciences (Bridging Post-doctoral Fellowship to LHP), the EJ Whitten Foundation, the Peter and Lyndy White Foundation and TissuPath Pathology. The financial support for establishing new PDXs was provided by the Movember Foundation, as a project of the Global Action Plan 1 (GAP1) PDX project.

References

1. Gao H, Korn JM, Ferretti S, Monahan JE, Wang Y, Singh M, Zhang C, Schnell C, Yang G, Zhang Y, Balbin OA, Barbe S, Cai H, Casey F, Chatterjee S, Chiang DY, Chuai S, Cogan SM, Collins SD, Dammassa E, Ebel N, Embry M, Green J, Kauffmann A, Kowal C, Leary RJ, Lehar J, Liang Y, Loo A,

- Lorenzana E, Robert McDonald Iii E, McLaughlin ME, Merkin J, Meyer R, Naylor TL, Patawaran M, Reddy A, Röelli C, Ruddy DA, Salangsang F, Santacroce F, Singh AP, Tang Y, Tinetto W, Tobler S, Velazquez R, Venkatesan K, Von Arx F, Wang HQ, Wang Z, Wiesmann M, Wyss D, Xu F, Bitter H, Atadja P, Lees E, Hofmann F, Li E, Keen N, Cozens R, Jensen MR, Pryer NK, Williams JA, Sellers WR. High-throughput screening using patient-derived tumor xenografts to predict clinical trial drug response. *Nat Med*. 2015;21:1318.
2. Bult CJ, Airhart SD, Chuang J, Gandour-Edwards R, George J, Graber J, Karuturi RKM, Keck J, Kim H, Lara P, Li T, Mack PC, Shultz L, Tepper C, Burich R, Woo XY, Yang Y, de Vere White R, Gandara DR, Liu ET. The JAX patient-derived xenograft program: A unique resource to advance genome-guided cancer medicine and therapeutic agent testing. *J Clin Oncol*. 2014;32(15_suppl):e22151-e22151.
3. Byrne AT, Alf  rez DG, Amant F, Annibali D, Arribas J, Biankin AV, Bruna A, Budinsk   E, Caldas C, Chang DK, Clarke RB, Clevers H, Coukos G, Dangles-Marie V, Eckhardt SG, Gonzalez-Suarez E, Hermans E, Hidalgo M, Jarzabek MA, de Jong S, Jonkers J, Kemper K, Lanfranccone L, M  landsmo GM, Marangoni E, Marine J-C, Medico E, Norum JH, Palmer HG, Peeper DS, Pelicci PG, Piris-Gimenez A, Roman-Roman S, Rueda OM, Seoane J, Serra V, Soucek L, Vanhecke D, Villanueva A, Vinolo E, Bertotti A, Trusolino L. Interrogating open issues in cancer precision medicine with patient-derived xenografts. *Nature Reviews Cancer*. 2017;17:254.

4. Navone NM, van Weerden WM, Vessella RL, Williams ED, Wang Y, Isaacs JT, Nguyen HM, Culig Z, van der Pluijm G, Rentsch CA, Marques RB, de Ridder CMA, Bubendorf L, Thalmann GN, Brennen WN, Santer FR, Moser PL, Shepherd P, Efsthathiou E, Xue H, Lin D, Collins A, Maitland N, Buzza M, Kouspou M, Achtman A, Taylor RA, Risbridger G, Corey E. Movember GAP1 PDX project: An international collection of serially transplantable prostate cancer patient-derived xenograft (PDX) models. *The Prostate*. 2018;78(16):1262-1282.

5. Lawrence MG, Obinata D, Sandhu S, Selth LA, Wong SQ, Porter LH, Lister N, Pook D, Pezaro C, Goode DL, Rebello R, Clark AK, Papargiris M, Van Gramberg J, Banks P, Wang H, Niranjana B, Keerthikumar S, Hedwards SL, Huglo A, Yang R, Henzler C, Li Y, Lopez-Campos F, Castro E, Toivanen R, Azad AA, Bolton D, Goad J, Grummet J, Harewood L, Kourambas J, Lawrentschuk N, Mood D, Murphy DG, Sengupta S, Snow R, Thorne H, Mitchell C, Pedersen J, Clouston D, Norden S, Ryan A, Dehm SM, Tilley WD, Pearson RB, Hannan RD, Frydenberg M, Furic L, Taylor RA, Risbridger GP. Patient-derived models of abiraterone and enzalutamide-resistant prostate cancer reveal sensitivity to ribosome-directed therapy. *Eur Urol*. 2018;74(5):562-572.

6. Nguyen HM, Vessella RL, Morrissey C, Brown LG, Coleman IM, Higano CS, Mostaghel EA, Zhang X, True LD, Lam HM, Roudier M, Lange PH, Nelson PS, Corey E. LuCaP prostate cancer patient-derived xenografts reflect the molecular heterogeneity of advanced disease and serve as models for evaluating cancer therapeutics. *The Prostate*. 2017;77(6):654-671.

7. Lin D, Wyatt AW, Xue H, Wang Y, Dong X, Haegert A, Wu R, Brahmbhatt S, Mo F, Jong L, Bell RH, Anderson S, Hurtado-Coll A, Fazli L, Sharma M, Beltran H, Rubin M, Cox M, Gout PW, Morris J, Goldenberg L, Volik SV, Gleave ME, Collins CC, Wang Y. High Fidelity Patient-Derived Xenografts for Accelerating Prostate Cancer Discovery and Drug Development. *Cancer Res.* 2014;74(4):1272-1283.
8. Lange T, Oh-Hohenhorst SJ, Joosse SA, Pantel K, Hahn O, Gosau T, Dyshlovoy SA, Wellbrock J, Feldhaus S, Maar H, Gehrcke R, Kluth M, Simon R, Schlomm T, Huland H, Schumacher U. Development and Characterization of a Spontaneously Metastatic Patient-Derived Xenograft Model of Human Prostate Cancer. *Scientific reports.* 2018;8(1):17535-17535.
9. Niranjan B, Lawrence MG, Papargiris MM, Richards MG, Hussain S, Frydenberg M, Pedersen J, Taylor RA, Risbridger GP. Primary culture and propagation of human prostate epithelial cells. *Methods Mol Biol.* 2013;945:365-382.
10. Han S-H, Shim S, Kim M-J, Shin H-Y, Jang W-S, Lee S-J, Jin Y-W, Lee S-S, Lee SB, Park S. Long-term culture-induced phenotypic difference and efficient cryopreservation of small intestinal organoids by treatment timing of Rho kinase inhibitor. *World J Gastroenterol.* 2017;23(6):964-975.
11. Liu X, Ory V, Chapman S, Yuan H, Albanese C, Kallakury B, Timofeeva OA, Nealon C, Dakic A, Simic V, Haddad BR, Rhim JS, Dritschilo A, Riegel A, McBride A, Schlegel R. ROCK Inhibitor and Feeder Cells Induce the Conditional Reprogramming of Epithelial Cells. *The American Journal of Pathology.* 2012;180(2):599-607.

12. Martin-Ibañez R, Unger C, Strömberg A, Baker D, Canals JM, Hovatta O. Novel cryopreservation method for dissociated human embryonic stem cells in the presence of a ROCK inhibitor. *Hum Reprod.* 2008;23(12):2744-2754.
13. Claassen DA, Desler MM, Rizzino A. ROCK inhibition enhances the recovery and growth of cryopreserved human embryonic stem cells and human induced pluripotent stem cells. *Mol Reprod Dev.* 2009;76(8):722-732.
14. Watanabe K, Ueno M, Kamiya D, Nishiyama A, Matsumura M, Wataya T, Takahashi JB, Nishikawa S, Nishikawa S-i, Muguruma K, Sasai Y. A ROCK inhibitor permits survival of dissociated human embryonic stem cells. *Nat Biotechnol.* 2007;25:681+.
15. Sato T, Vries RG, Snippert HJ, Van de Wetering M, Barker N, Stange DE, Van Es JH, Abo A, Kujala P, Peters PJ, Clevers H. Single Lgr5 stem cells build crypt-villus structures in vitro without a mesenchymal niche. *Nature.* 2009;459:262+.
16. Herraiz S, Novella-Maestre E, Rodríguez B, Díaz C, Sánchez-Serrano M, Mirabet V, Pellicer A. Improving ovarian tissue cryopreservation for oncologic patients: slow freezing versus vitrification, effect of different procedures and devices. *Fertility and Sterility.* 2014;101(3):775-784.e771.
17. Kaneko H, Kikuchi K, Nakai M, Somfai T, Noguchi J, Tanihara F, Ito J, Kashiwazaki N. Generation of live piglets for the first time using sperm retrieved from immature testicular tissue cryopreserved and grafted into nude mice. *PLoS ONE.* 2013;8(7).

18. Poels J, Van Langendonckt A, Many M-C, Wese F-X, Wyns C. Vitrification preserves proliferation capacity in human spermatogonia. *Hum Reprod.* 2013;28(3):578-589.
19. Alsop K, Thorne H, Sandhu S, Hamilton A, Mintoff C, Christie E, Spruyt O, Williams S, McNally O, Mileskin L, Ananda S, Hallo J, Loi S, Scott C, Savas P, Devereux L, O'Brien P, Gunawardena S, Hampson C, Strachan K, Jaravaza RD, Francis V, Young G, Ranson D, Samaranayake R, Stevens D, Boyle S, Fedele C, Topp M, Ho G, Teo ZL, Taylor RA, Papargiris MM, Lawrence MG, Wang H, Risbridger GP, Haynes NM, Medon M, Johnstone RW, Vidacs E, Arnau GM, Vergara IA, Papenfuss AT, McArthur G, Waring P, Carvosso S, Angel C, Gyorki D, Solomon B, Mitchell G, Shanley S, Francis PA, Dawson SJ, Haffenden A, Tidball E, Volchek M, Pyman J, Madadin M, Leditschke J, Cordner S, Melbourne Melanoma P, Australian Ovarian Cancer Study G, Kathleen Cuninghame Foundation Consortium for Research into Familial Breast C, Shackleton M, Bowtell DD. A community-based model of rapid autopsy in end-stage cancer patients. *Nat Biotechnol.* 2016;34(10):1010-1014.
20. Lawrence MG, Taylor RA, Toivanen R, Pedersen J, Norden S, Pook DW, Frydenberg M, Papargiris MM, Niranjana B, Richards MG, Wang H, Collins AT, Maitland NJ, Risbridger GP. A preclinical xenograft model of prostate cancer using human tumors. *Nat Protoc.* 2013;8(5):836-848.
21. Dalrymple SL, Becker RE, Isaacs JT. The quinoline-3-carboxamide anti-angiogenic agent, tasquinimod, enhances the anti-prostate cancer efficacy of

androgen ablation and taxotere without effecting serum PSA directly in human xenografts. *The Prostate*. 2007;67(7):790-797.

22. Nagabhushan M, Miller CM, Pretlow TP, Giaconia JM, Edgehouse NL, Schwartz S, Kung H-J, de Vere White RW, Gumerlock PH, Resnick MI, Amini SB, Pretlow TG. CWR22: The First Human Prostate Cancer Xenograft with Strongly Androgen-dependent and Relapsed Strains Both *in Vivo* and in Soft Agar. *Cancer Res*. 1996;56(13):3042-3046.
23. Kim D, Langmead B, Salzberg SL. HISAT: a fast spliced aligner with low memory requirements. *Nat Methods*. 2015;12(4):357-360.
24. Wakefield LM. Xenomapper: Mapping reads in a mixed species context. *The Journal of Open Source Software*. 2016;1(1).
25. Liao Y, Smyth GK, Shi W. The Subread aligner: fast, accurate and scalable read mapping by seed-and-vote. *Nucleic Acids Res*. 2013;41(10):e108.
26. Robinson MD, Oshlack A. A scaling normalization method for differential expression analysis of RNA-seq data. *Genome Biol*. 2010;11(3):R25.
27. Pretlow TG, Wolman SR, Micale MA, Pelley RJ, Kursh ED, Resnick MI, Bodner DR, Jacobberger JW, Delmoro CM, Giaconia JM, et al. Xenografts of primary human prostatic carcinoma. *J Natl Cancer Inst*. 1993;85(5):394-398.
28. Vernardis SI, Terzoudis K, Panoskaltsis N, Mantalaris A. Human embryonic and induced pluripotent stem cells maintain phenotype but alter their metabolism after exposure to ROCK inhibitor. *Scientific reports*. 2017;7:42138-42138.

29. Zhao M, Fan C, Ernst PJ, Tang Y, Zhu H, Mattapally S, Oduk Y, Borovjagin AV, Zhou L, Zhang J, Zhu W. Y-27632 preconditioning enhances transplantation of human-induced pluripotent stem cell-derived cardiomyocytes in myocardial infarction mice. *Cardiovasc Res*. 2019;115(2):343-356.
30. Risbridger GP, Toivanen R, Taylor RA. Preclinical Models of Prostate Cancer: Patient-Derived Xenografts, Organoids, and Other Explant Models. *Cold Spring Harbor Perspectives in Medicine*. 2018;8(8).
31. Risbridger GP, Lawrence MG. Towards best practice in establishing patient-derived xenografts. In: Wang Y, Lin D, Gout PW, eds. *Patient-derived xenograft models of human cancer*. Humana Press; 2017.
32. Rubin MA, Putzi M, Mucci N, Smith DC, Wojno K, Korenchuk S, Pienta KJ. Rapid ("warm") autopsy study for procurement of metastatic prostate cancer. *Clin Cancer Res*. 2000;6(3):1038-1045.
33. Presnell SC, Werdin ES, Maygarden S, Mohler JL, Smith GJ. Establishment of short-term primary human prostate xenografts for the study of prostate biology and cancer. *Am J Pathol*. 2001;159(3):855-860.
34. Lawrence MG, Pook DW, Wang H, Porter LH, Frydenberg M, Kourambas J, Appu S, Poole C, Beardsley EK, Ryan A, Norden S, Papargiris MM, Risbridger GP, Taylor RA. Establishment of primary patient-derived xenografts of palliative TURP specimens to study castrate-resistant prostate cancer. *Prostate*. 2015;75(13):1475-1483.

Figure Legends

Fig. 1. Patient-derived xenografts (PDXs) of prostate cancer can be re-established following cryopreservation using slow freezing protocols. (A) PDX 27.1 was established as a serially-transplantable PDX from a prostate cancer dural metastasis. PDX tissue was either re-grafted directly into host mice as fresh tissue or cryopreserved using one of three cryopreservation protocols: slowing freezing in fetal calf serum supplemented with dimethyl sulfoxide (DMSO; designated FCS), slow freezing in fetal calf serum supplemented with DMSO and Rho-associated kinase inhibitor (designated FCS-R) or vitrification. **(B)** The volume of grafts harvested six weeks after implantation. Samples were grafted into host mice as fresh tissue ($n = 3$) or following cryopreservation with FCS ($n = 6$), FCS-R ($n = 6$) or vitrification (V; $n = 6$). **(C)** Hematoxylin and eosin (H&E) staining and immunohistochemical staining for luminal cell marker cytokeratin 8/18 (ck8/18), androgen receptor (AR), prostate specific antigen (PSA), Ki67 and cleaved caspase 3 (CC3) in xenografts. **(D,E)** Average percentage of Ki67-positive cells **(D)** and cleaved caspase 3-positive (CC3) cells **(E)** in freshly grafted controls ($n = 3$) or in grafts cryopreserved with FCS ($n = 6$), FCS-R ($n = 6$) or vitrification (V; $n = 6$). * $P < 0.05$, ** $P < 0.01$, *** $P < 0.001$ as determined by one-way ANOVA with post hoc Dunnett's test. All data are expressed as mean \pm SEM. Scale bars = 50 μ M.

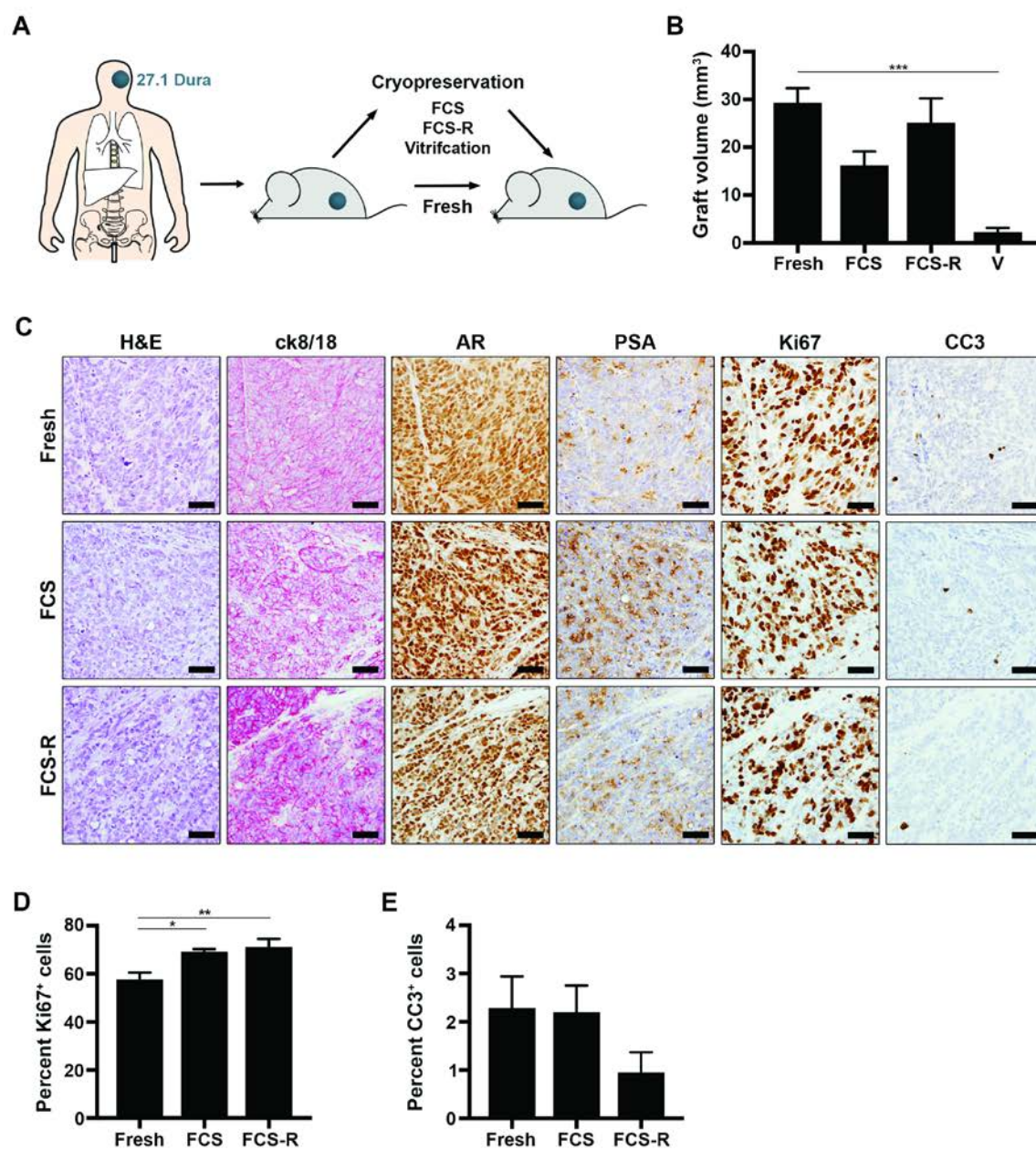


Fig. 2. Patient-derived xenografts maintain the same growth rate following cryopreservation. (A-I) Growth rate of nine PDXs grown in host mice supplemented with testosterone before cryopreservation (grey), in the first transition generation immediately after being re-established from cryopreserved tissue (orange) and subsequent generations after cryopreservation (black). Each step represents a new generation where graft volume increased by at least 10 fold between tissue implantation and collection. PDXs were cryopreserved using the slow freezing protocol in fetal calf serum with 10% DMSO and Rho-associated kinase inhibitor (FCS-R) before being re-established in host mice (arrow). (F) The average number of days per generation in nine PDX lines before cryopreservation ($n = 9$), in the first transition generation after cryopreservation ($n = 9$) and after cryopreservation ($n = 8$) in FCS-R. Data are expressed as mean \pm SEM, one-way ANOVA with post hoc Tukey's test, not significant).

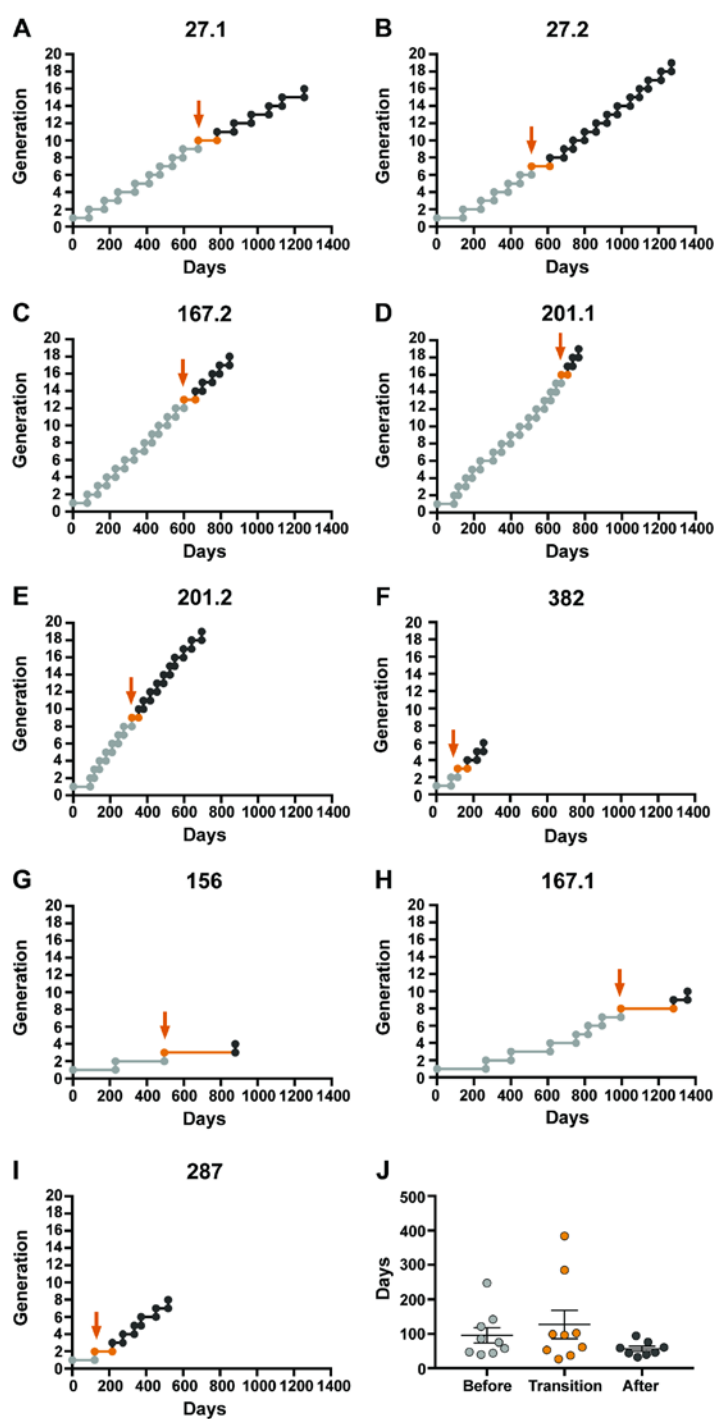


Fig. 3. Histological features and the transcriptome profile of patient-derived xenografts (PDXs) are maintained following cryopreservation. (A) Hematoxylin and eosin staining of nine PDXs, grown in testosterone-supplemented host mice, before and after slow freezing cryopreservation in fetal calf serum with 10% DMSO and Rho-associated kinase inhibitor. Scale bars = 50 μ m. (B) Scatter plots displaying the log₂ normalized transcript counts (in counts per million) per gene in three generations of PDX tumor tissue prior to cryopreservation (generation 1, 5 and 8) compared to one generation of PDX tumor tissue collected after cryopreservation (generation 14) for PDX 167.2, based on RNA sequencing. (C) Heatmap showing the Pearson's correlation coefficient between the transcriptome profiles of all pairs of samples for PDX 167.2, based on RNA sequencing.

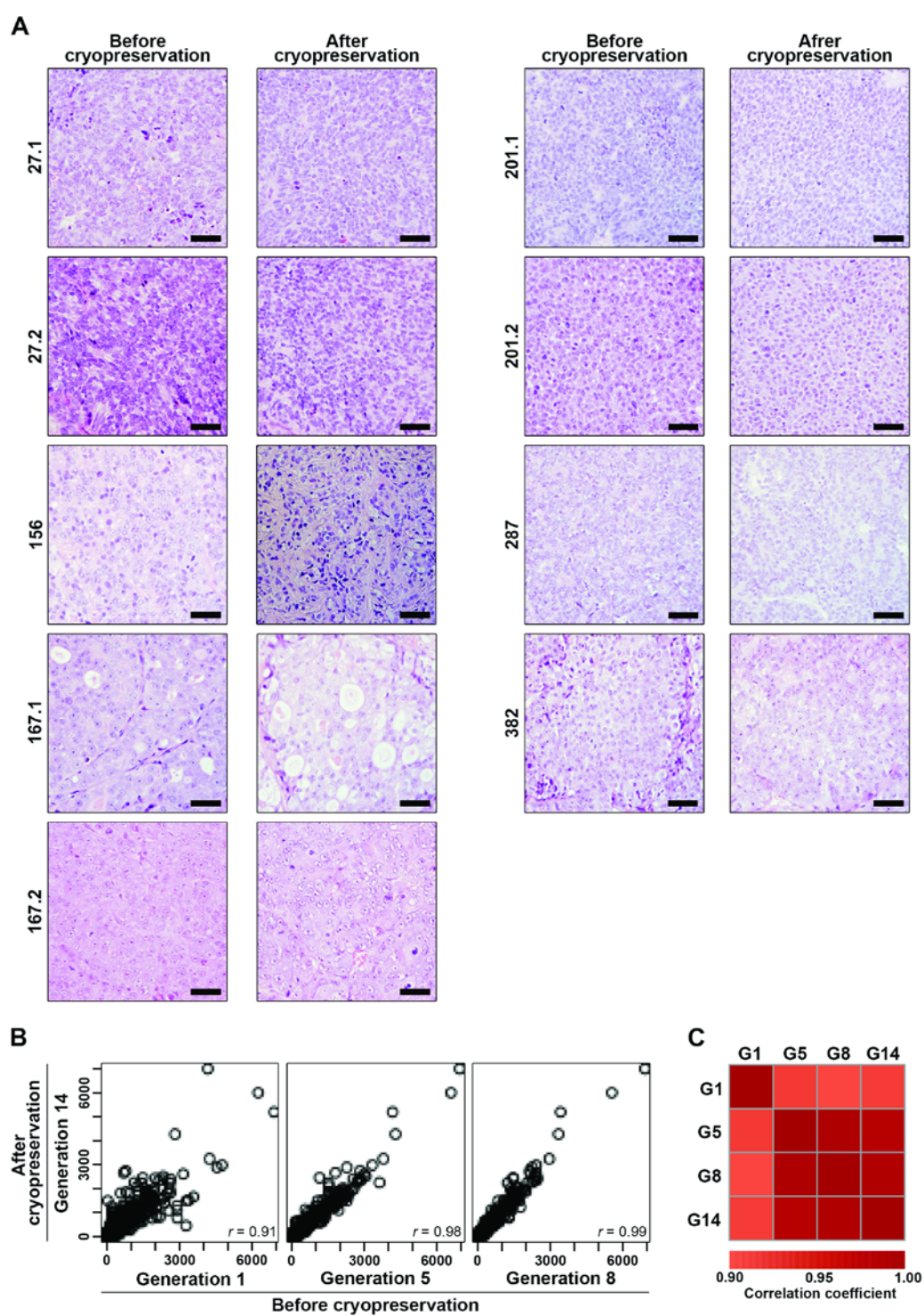


Table 1. Re-establishment of patient-derived xenografts after cryopreservation.

PDX ID	Sample type	Specimen	Clinical state	Host conditions	PDX generation cryopreserved	Time cryopreserved (days)	Tumor take rate following cryopreservation		
							FC S	FCS -R	V
27.1 ^a	Autopsy	Dural metastasis	Castrate-resistant	+T	1 ^b ; 9 ^c	21 ^b ; 212 ^c	100 (6/6) ^b	100% (6/6) ^b , 100% (5/5) ^c	50% (3/6) ^b
27.2 ^a	Autopsy	Lymph node metastasis	Castrate-resistant	+T	6 ^c	159 ^c	n/a	100% (6/6) ^c	n/a
				Castrate	Cx4 ^{c,d}	65 ^c	n/a	100% (4/4) ^c	n/a
156	Radical prostatectomy	Primary tumor	Hormone-naïve	+T	2 ^c	940 ^c	n/a	13% (1/8) ^c	n/a
167.1	Radical prostatectomy	Primary tumor	Hormone-naïve	+T	7 ^c	374 ^c	n/a	17% (1/6) ^c	n/a
167.2 ^a	Palliative surgery	Spine metastasis	Castrate-resistant	+T	12 ^c	48 ^c	n/a	100% (4/4) ^c	n/a
201.1 ^a	Autopsy	Dural metastasis	Castrate-resistant	+T	16 ^c	819 ^c	n/a	100% (6/6) ^c	n/a
				Castrate	Cx7 ^{c,d}	91 ^c	n/a	100% (4/4) ^c	n/a
201.2 ^a	Autopsy	Lung metastasis	Castrate-resistant	+T	8 ^c	144 ^c	n/a	100% (7/7) ^c	n/a
				Castrate	Cx1 ^{c,d}	90 ^c	n/a	100% (4/4) ^c	n/a
287	Radical prostatectomy	Primary tumor	Hormone-naïve	+T	1 ^c	294 ^c	n/a	100% (5/5) ^c	n/a
382 ^a	Biopsy	Liver metastasis	Castrate-resistant	+T	2 ^c	325 ^c	n/a	100% (7/7) ^c	n/a

^aPreviously published in Lawrence et al. 2018 [5].

^bComparison of cryopreservation protocols.

^cRe-establishment of patient-derived xenograft lines following cryopreservation.

^dNumber of generations in castrated host mice.

1.1 Tumor take rate shows the percentage of xenografts which successfully re-established following cryopreservation and contained viable tumor tissue. The number of xenografts containing tumor/total number of xenografts implanted is shown in brackets. Abbreviations: Cx, castrate; FCS, slow freezing cryopreservation protocol in fetal calf serum with 10% DMSO; FCS-R, slow freezing cryopreservation protocol in fetal calf serum with 10% DMSO and Rho associated kinase inhibitor; n/a, not applicable; PDX, patient-derived xenograft; +T, supplemented with testosterone; V, vitrification cryopreservation protocol.